Environmental
Science
Advances

Dredged Sludge Residual Water

Treated Effluent

Ecological Recovery & Sustainability

High Removal Efficiency

ROYAL SOCIETY
OF CHEMISTRY

PAPER
Jun Li, Salma Tabassum *et al.*
Integrated magnetic flocculation-horizontal tube
sedimentation process for treating dredging residual water:
environmental restoration of Wolong Lake

Environmental Science Advances

Check for updates

Integrated magnetic flocculation-horizontal tube sedimentation process for treating dredging residual water: environmental restoration of Wolong Lake

Jun Li,*[a] Salma Tabassum [ID] *[bc] and Imran Khan [ID] [d]

Residual water from dredging contains high concentrations of heavy metals, causing severe environmental pollution in lakes. The present study develops integrated magnetic flocculation-horizontal tube sedimentation equipment. In the Wolong Lake region of China, the impact of treatment with the device on the residual water from dredged sludge under various inlet water flows was investigated. In a single-factor experiment, flocculants such as polyaluminum chloride (PAC), polymeric ferric sulfate (PFS), ferric chloride (FeCl$_3$), and aluminum sulphate (Al$_2$(SO$_4$)$_3$) were used at doses of 20–120 mg L^{-1} to treat the residual water from dredged sludge. The residual wastewater from dredged sludge was best treated with PAC at 60 mg L; the removal efficiency of suspended solids (SS), chemical oxygen demand (COD), total phosphorous (TP), and ammonia nitrogen (NH$_3$-N) were (81.37 ± 1.66)%, (44.65 ± 2.31)%, (76.48 ± 1.08)%, and (17.64 ± 0.85)%, respectively. The pollutants in the water were further removed using magnetic flocculation (single-factor test and orthogonal analysis). The response surface method was used to optimize the PAC, magnetic powder, and polyacrylamide (PAM) doses to achieve 93.1% SS, 91.2% TP, and 71.2% COD removal. The device was operated for 30 consecutive days at various water intake volumes (4, 6, and 8 m^3 h^{-1}). The residual water's COD, SS, TP, and NH$_3$-N levels effectively meet the environmental quality standards for surface water. With SpaceClaim as the pre-processing software and Fluent as the solver, a computational fluid dynamics (CFD) simulation analysis of the test device was conducted. CFD validations confirmed the design reliability. The reliability and rationality of the test device's operation were verified through simulation and analysis using the dual Euler model. The circular treatment design has significant environmental implications in restoring the ecological balance of the Wolong Lake Wetland.

Environmental significance

The Wolong Lake wetland ecosystem is rich in natural resources and has multiple ecological functions. However, the pollutants in the Wolong Lake sediment are released and migrate back into the water under certain conditions, causing endogenous pollution of the water body. This study developed an integrated flocculation-sedimentation sewage treatment equipment based on magnetic flocculation technology and a horizontal tube sedimentation process. The system was used to treat dredged sludge residual water for the environmental protection dredging project in the Wolong Lake area. By examining the impact of various factors on the flocculation effect and observing the removal of different pollutants during actual operation, the optimized treatment of the dredged sludge residual water from Wolong Lake generates water that meets the surface water environmental quality standard.

1 Introduction

Environmentally friendly dredging is a crucial measure for the ecological management of lakes and reservoirs, playing a vital role in water environment management and restoration. However, this method produces large amounts of dredged sediment, resulting in large amounts of mud. During this process, the treated mud is deposited at the bottom of the mud disposal site, and excess water flows out from the site, referred to as dredging residual water. This residual water contains high concentrations of heavy metals, causing severe environmental pollution.[1] This imposes high requirements for properly treating residual water after environmental dredging and preventing secondary pollution.[2]

The treatment of residual water from dredged sludge primarily involves physical and chemical treatment. In the

[a]*School of Municipal and Environmental Engineering, Shenyang Jianzhu University, Shenyang 110168, China. E-mail: junlee@sjzu.edu.cn*

[b]*Department of Chemistry, Faculty of Science, Sakarya University, Sakarya 54187, Turkiye. E-mail: tsalma@sakarya.edu.tr; salmazenith@gmail.com*

[c]*Biomedical, Magnetic and Semiconductor Materials Research Center (BIMAS-RC), Sakarya University, Sakarya 54187, Turkiye*

[d]*Department of Chemistry, College of Science, Sultan Qaboos University, Muscat, Oman*

© 2026 The Author(s). Published by the Royal Society of Chemistry

Environ. Sci.: Adv., 2026, 5, 753–771 | **753**

physical treatment method, residual water treatment is primarily achieved by controlling the residence time of residual water, the water depth of the water surface, and the speed of water flow. In the case of environmentally friendly dredging, it must be carried out in a place with a large water capacity.[3] Chemical reagents are used to treat residual water. A certain amount of flocculant is added to the residual water in proportion. The flocculant effectively adsorbs pollutants in the water, thereby reducing the concentration of contaminants in the remaining water.[4] The selection of flocculants in the flocculation method is directly related to the final effect of water pollutant removal.[5,6] Coagulation and precipitation are examples of environmental technologies that could be used to settle fine particles. However, large settling tanks and coagulants are required for the procedure. Hong et al.[7] investigated the use of magnetic separation for the rapid settling of fine particles suspended during the dredging process. For the quick settling of fine particles suspended during the dredging process, magnetic separation is employed. The application of a magnetic force increases the settling velocity, and the accelerated settling process can reduce the required volume of the settling tank, which is usually located on a ship for dredging. The magnetic-assisted settling also reduces the release of heavy metals through the turbid water by precipitating highly polluting particles with magnetic force.[7]

Compared to traditional water-treatment methods, magnetic flocculation is simple, safe to operate, easy to maintain, has high processing efficiency,[8] a good treatment effect,[9,10] lower costs, a smaller footprint, can withstand load impacts, and is less affected by water temperature and climate.[11,12] Magnetic flocculation technology combines a magnetic field with the flocculation process, requiring consideration of both physical and chemical factors in water treatment projects. These factors include hydraulic conditions, magnetic field strength, flocculant dosage (magnetic powder), and reaction pH.[13–15] Adjusting these parameters can affect the degree of contact between the flocculant and the colloidal particles, as well as the strength of the formed magnetic flocculation entities.[16] The horizontal tube precipitation and separation device is a sedimentation tank with high precipitation efficiency, good operational stability, strong adaptability, and a more flexible design.[17,18] In actual engineering applications, horizontal tube sedimentation tanks can treat low-temperature, low-turbidity raw water and high-turbidity raw water, as well as high-temperature and high-algae raw water.[19] A horizontal tube sedimentation tank is more conducive to optimizing the treatment effect of the sewage treatment plant than other high-efficiency sedimentation tanks.[20] Computational fluid dynamics (CFD) has been effectively utilized to demonstrate the limitations of the average velocity gradient approach in classifying a flocculator. Robust coupling of population balance modelling for flocculation processes with CFD has advanced wastewater flocculation.[21] Compared to primary decantation, dissolved air flotation (DAF) offers higher efficiency, requires less space, and provides greater flexibility. However, it also has some disadvantages, such as high costs, energy requirements (including pressure pumps, motors, air compressors, and mechanical systems), and

the need for chemicals.[22] The selection of a set of design and operating parameters for a DAF is directly related to the characteristics of the wastewater.[23]

The integration of magnetic flocculation and horizontal tube sedimentation as a field-scale innovation design described in this study increases the flexibility of the process, saves land area, and is beneficial for dredging residual water treatment.

Wolong Lake is a provincial waterfowl habitat and aquatic resources protection wetland lake in China. The Lake has a basin area of 1592 square kilometers, a water surface area of about 60 square kilometers, and a circumference of 55 kilometers. The maximum water storage capacity is approximately 100 million cubic meters, and the average water depth ranges from 1.5 to 2 meters.[24] The quality of Wolong's lake water deteriorates if residual water is released directly into the Lake. The mechanism of flocculants has not been comprehensively investigated to date. The current conditions for improving water quality in Wolong Lake are relatively high, but the water quality in some areas is still poor. Combined with sediment dredging and dewatering activities, as well as the use of flocculants, the quality of the treated sediment residual water may decline. Directly releasing this residual water into Wolong Lake could further reduce the Lake's water quality. Therefore, selecting an effective residual water treatment technology is crucial. The intricate and unique nature of the flocs formed is attributed to the diversity of pollution components and the environmental characteristics of different regions. To address this issue, a purification test was conducted on the residual water in Wolong Lake after the dehydration of the polluted bottom sludge.

The objective of the current study was to achieve water quality indicators that met the discharge standards before the residual water was discharged. A residual water purification treatment test was conducted on the polluted residual water after dehydration of the polluted bottom sludge in Wolong Lake waters to assess whether a high-standard discharge following residual water treatment was achieved. This study aims to develop flocculation-sedimentation integrated sewage treatment equipment suitable for use with residual water from dredged sludge in lakes. By analyzing the physical and chemical properties of dredged sludge residual water and adjusting the combination of different flocculants, magnetic powder, and coagulant aids, we explore the optimal flocculation reaction dosage combination and determine its ideal usage conditions, serving as a guide for more in-depth research. The main objectives of this study were: (i) to investigate the flocculation effect of flocculants on dredging residual water at different dosages. Comparative tests were conducted on flocculants, including PAC, PFS, $FeCl_3$, and aluminum sulfate, as they are commonly used inorganic coagulants. Due to its good flocculation effect and low cost, this approach is widely used in various water treatment processes in practical applications. The optimal dosage of each flocculant was determined for comparison and selection. The optimal flocculant type was selected through comprehensive analysis; (ii) magnetic powder was added to conduct a magnetic flocculation test, and the best flocculant was selected. The results were combined to consider the removal efficiency of suspended solids, total phosphorus, COD, and other indicators, as well as factors such as the economy and operability

of practical applications. Experiments were conducted to study the dosage of magnetic powder, particle size of the magnetic powder, coagulant PAM dosage, drug dosage sequence, and stirring water hydraulic conditions; (iii) the PAC dosage, PAM dosage, and magnetic powder dosage were selected as independent variables according to the single-factor test results, and the Box–Behnken model was used to design a response surface test to examine the interaction between factors; (iv) the integrated flocculation-sedimentation device was used to explore the removal effect of the device on major pollutants in the residual water under actual operating conditions; and (v) CFD numerical simulations were carried out to verify the rationality and reliability of the operation of the test device.

2 Materials and methods

2.1 Experimental drugs

Polyacrylamide (PAM), polyaluminum chloride (PAC: content $\geq 27.0\%$; pH 3.5–5.0 in 1% aqueous solution), aluminum sulfate $(Al_2(SO_4)_3)$, and ferric chloride $(FeCl_3)$ were analytical grade, and the highest level of purity was used. The main component of the magnetic powder used in this experiment was Fe_3O_4. The magnetic powder used in the test was purchased as a finished product, and no material testing data are available. Magnetic powder with a ferric oxide content of greater than 97% was used (insoluble in water). Fe_3O_4, as a magnetic powder, can be recycled after the test and can be recovered approximately 15 times.[25] Chemical substances, except for magnetic powder, were prepared as solutions first to facilitate subsequent test operations.

2.2 Operational strategies based on traditional flocculation: dredged sludge residual water

Four commonly used inorganic flocculants, PAC, PFS, $FeCl_3$, and $Al_2(SO_4)_3$, were tested to investigate the flocculation effect of these flocculants at various dosages in treating the dredged sludge residual water of Wolong Lake and to determine the respective characteristics of each flocculant. 200 mL of the solution to be tested was added to a 250 mL beaker. The pre-prepared coagulant at concentrations of 20, 40, 60, 80, 100, and 120 mg L^{-1} was added to a beaker under rapid stirring. The mixture was stirred under fast stirring conditions (2 minutes, 200 r min^{-1}) and then under slow stirring conditions (5 minutes, 60 r min^{-1}). The supernatant (settled for 20 minutes) was taken 2 cm below the liquid level, and the concentration of contaminants was measured. The residual water extracted from the bottom mud in the ecological protection region of Wolong Lake following environmental dredging was subjected to a comprehensive physical and chemical property investigation (pH 7–8, COD 50–70 mg L^{-1}, TP 0.2–0.4 mg L^{-1}, NH_3-N 1.1–1.3 mg L^{-1}, and SS 150–170 mg L^{-1}).

2.3 Magnetic flocculation tests

COD, SS, TP, and NH_3-N were used as indicators to examine the effects of magnetic powder dosage, magnetic powder particle size, PAM dosage, and hydraulic conditions on the magnetic

flocculation effect through a single-factor experiment, and the dosage was optimized through the response surface to obtain the optimal dosage of chemicals for magnetic flocculation. The results pave the way for further research on the design and operation of the integrated flocculation-sedimentation device. To examine the effect of magnetic powder dosage, 200 mL of the solution was added to a 250 mL beaker. The pre-prepared PAC solution at concentrations of 0, 50, 60, 100, 150, 200, and 250 mg L^{-1} was added to the beaker under both rapid and slow stirring conditions. The supernatant (settled for 20 minutes) was taken 2 cm below the liquid level, and the concentration of contaminants was measured. The PAC and magnetic powder dosages were maintained at 60 mg L^{-1} and 100 mg L^{-1}, respectively. Several common magnetic powders with different particle sizes (18.7, 25, 45, and 75 µm) were selected for testing. For the effect of PAM dosage, 200 mL of the solution was transferred to a 250 mL beaker. The pre-prepared PAC solution (60 mg L^{-1}) and magnetic powder (100 mg L^{-1}) were added to the beaker under rapid stirring, then 0, 0.5, 1, 1.5, 2.0, and 2.5 mg L^{-1} PAM were added under slow stirring conditions. The supernatant (settled for 20 minutes) was taken 2 cm below the liquid level, and the concentration of the contaminants was measured (pH 7.0 ± 0.5 and temperature 15 °C $\pm$ 5 °C). The detection limits and standard deviations for COD, TP, and NH_3-N measurements were NH_3-N (0–2.0 mg L^{-1}): $y = (5.65385 \pm 0.04901)x + (-0.01097 \pm 0.00896)$, $R^2 = 0.99955$; TP (0–0.6 mg L^{-1}): $y = (2.71233 \pm 0.02135)x + (0.00041 \pm 0.00011)$, $R^2 = 0.99963$; and COD (5–50 mg L^{-1}): $y = (6257.68293 \pm 63.69683)x + (0.52335 \pm 0.26365)$, $R^2 = 0.99928$.

2.4 Analytical methods

COD (potassium dichromate method), ammonia nitrogen (Nessler's reagent method), total phosphorus (ammonium molybdate method), and suspended solids (gravimetric method) were measured according to standard methods.[26] The schematic process flow diagram is shown in Scheme 1.

3 Results and discussion

3.1 Optimal dosage of different flocculants on dredged sludge residual water

The treatment effects of different flocculants on the residual water from Wolong Lake dredged sludge under their respective optimal dosage conditions are shown in Table 1 (SI Section 1). The test results show that at the respective optimum dosages the three flocculants (PAC, $Al_2(SO_4)_3$ and $FeCl_3$) had similar ammonia nitrogen removal efficiency ranging from 15.35% to 17.83% (PAC 17.64% $\pm$ 0.85% and $FeCl_3$ 17.83% $\pm$ 0.56%) and COD removal efficiency ranged from 41.83% to 44.65% (PAC 44.65% $\pm$ 2.31% and $Al_2(SO_4)_3$ 42.65% $\pm$ 1.55%). SS removal

Schematic process flow

Scheme 1

© 2026 The Author(s). Published by the Royal Society of Chemistry

Environ. Sci.: Adv., 2026, **5**, 753–771 | **755**

Table 1 Effects of different flocculants on the treatment of dredged sludge residual water

Flocculants	Dosage mg L^{-1}	COD removal efficiency %	SS removal efficiency %	TP removal efficiency %	NH$_3$-N removal efficiency %
PAC	60	44.65 ± 2.31	81.37 ± 1.66	76.48 ± 1.08	17.64 ± 0.85
Ferric chloride	40	42.55 ± 1.55	75.45 ± 2.56	83.86 ± 2.80	17.83 ± 0.56
Aluminum sulfate	60	42.65 ± 1.36	72.06 ± 2.95	81.63 ± 3.22	15.72 ± 1.16
PFS	80	41.83 ± 1.89	70.67 ± 1.47	81.44 ± 2.06	15.35 ± 1.35

efficiency varies significantly, ranging from 70.67% to 81.37% (PAC: 81.37% ± 1.66% and FeCl$_3$: 75.45% ± 2.56%). The TP removal efficiency ranged from 76.48% to 83.86% (FeCl$_3$ 83.86% ± 2.80% and Al$_2$(SO$_4$)$_3$ 81.63% ± 3.22%). PAC's flocculation effect was better overall than that of Al$_2$(SO$_4$)$_3$, FeCl$_3$ and PFS. PAC exhibited an excellent coagulation effect, producing less sludge during the coagulation process compared to the other three flocculants, which can reduce subsequent treatment costs.[27] PAC showed the best comprehensive coagulation performance by combining the various properties of these four inorganic flocculants. Therefore, PAC was selected as the coagulant to treat the residual water from the dredged sludge at Wolong Lake.

3.2 Magnetic flocculation tests

3.2.1 Effect of magnetic powder dosage. The analysis in Fig. 1(a–d) shows that the introduction of magnetic particles significantly improved pollutant removal efficiency. As the amount of magnetic powder was increased, the COD and SS removal efficiencies showed an increasing trend and later decreased. In contrast, the removal efficiencies of NH$_3$-N and TP showed only a slight variation. Specifically, when the magnetic powder was added at a concentration of 100 mg L^{-1}, the COD removal efficiency increased significantly from 44.56% ± 1.43% without magnetic powder addition to 62.83% ± 0.86%. The SS removal efficiency reached an optimal level of 87.25% ± 0.54%, while the TP removal efficiency gradually increased slightly with the increase in the amount of magnetic powder, up to 200 mg L^{-1}, then reached a peak. The NH$_3$-N removal efficiency was similar to that of TP. The removal efficiency was the highest when the added magnetic powder concentration was 150 mg L^{-1}. The addition of magnetic powder significantly enhanced the treatment effect of the flocculation process, effectively shortening the settling time and increasing the flocculation speed.[28] Magnetic powder and PAC interact during the rapid stirring stage, utilizing their respective flocculation competencies to form magnetic flocs with the magnetic powder at the core. This type of magnetic floc effectively aggregates destabilized particles and forms more compact structures under the influence of a magnetic field. Although increasing the amount of magnetic powder leads to a relative increase in turbidity, it can also increase the total concentration of particles in the water, thereby increasing the likelihood of particle encounters during the stirring process.[29] COD and SS removal efficiency by PAC flocculants was effectively improved by adding magnetic powder to the water samples. The test results

indicated that the higher the amount of magnetic powder used, the higher its efficiency in removing pollutants.

When the magnetic powder dosage exceeds the optimal dosage, the excess magnetic powder disperses in the water. It fails to effectively combine with the flocs, thus reducing the removal efficiency of pollutants and causing additional pollution in the water samples.[30] The combination of magnetic powder and pollutants in the water achieved an optimal effect at 100 mg L^{-1}, ensuring efficient removal of pollutants and minimizing the waste of magnetic powder and potential side effects.

3.2.2 Effect of magnetic powder particle size. The results showed that COD, TP, and SS pollutant concentrations initially increased and then decreased with the increase in magnetic powder particle size. The results are shown in Fig. 1(e–h); the abscissa represents the different particle sizes of the added magnetic powder, and the ordinate represents the corresponding pollutant removal efficiency. A comprehensive analysis revealed that when the magnetic particle size was 45 μm, the removal effect was optimal, with removal efficiencies of 89.48% ± 0.61%, 65.45% ± 0.30%, 89.52% ± 0.85% and 19.85% ± 0.28% for SS, COD, TP, and NH$_3$-N, respectively. The removal efficiency of pollutants in water generally begins to decrease when the magnetic particle size exceeds 45 μm. When the magnetic powder particle size is too small, the inertial collision shear force generated between the fine magnetic powder particles is too large, which can easily damage the already formed magnetic flocs and affect the treatment effect. When the magnetic powder particles are too large, it is observed that many magnetic powders sink to the bottom before mixing with the suspended matter in the raw water, which not only leads to a waste of magnetic powder but also affects the water discharge effect.[31] Therefore, the optimal particle size of magnetic powder was determined to be 45 μm.

3.2.3 Effect of PAM dosage. Experimental observations showed that adding coagulant alone, even with the optimal flocculation dosage of PAC, results in relatively slow floc formation. When the flocs formed were too large, it was observed that many magnetic powders sank to the bottom before mixing with the suspended matter in the raw water. It caused a waste of magnetic powder and affected the water discharge effect. Therefore, the optimal particle size of magnetic powder was determined to be 45 μm. The structure was often loose, and sedimentation was slow, so the solid–liquid interface was unclear after sedimentation. PAM can be introduced as a flocculant at the end of the rapid mixing stage to enhance the flocculation effect. PAM and PAC worked
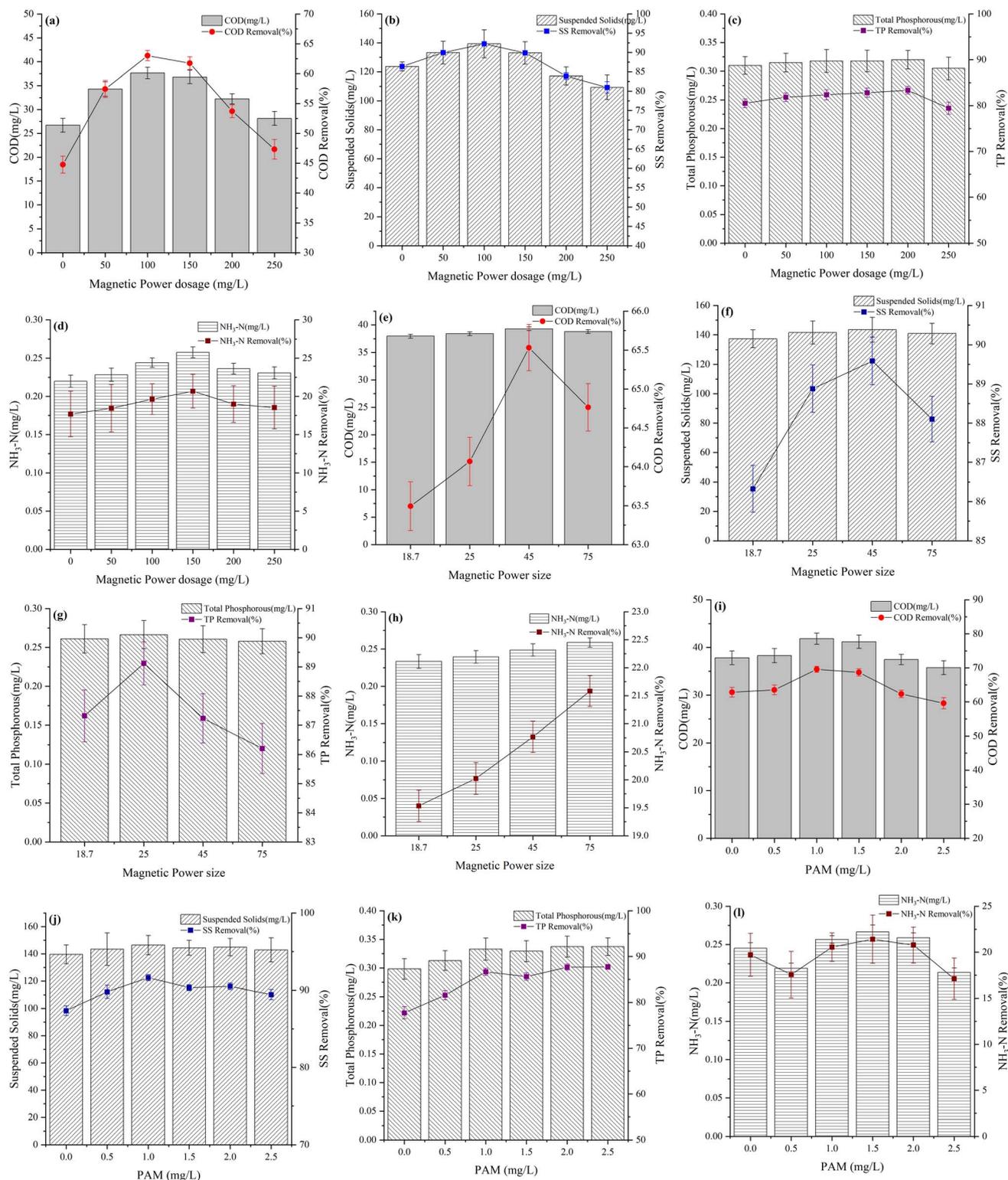
Fig. 1 Removal efficiency of various pollutants by magnetic powder with (a) COD, (b) SS, (c) TP, and (d) NH$_3$$^-$N, magnetic particles (different particle sizes): (e) COD, (f) SS, (g) TP, (h) NH$_3$$^-$N; and polyacrylamide with (i) COD, (j) SS, (k) TP, and (l) NH$_3$$^-$.

synergistically to produce a better flocculation effect. PAM is a high-molecular-weight polymer with a long-chain structure that primarily functions through its long chains for adsorption bridging. PAM addition under rapid mixing conditions disrupts its structure, causing the shortening of molecular chains and adversely affecting flocculation efficiency. As a result, the timing of the PAM addition is crucial.[32] The introduction of PAM after the initial flocculation process of PAC in the rapid mixing stage

can reduce the impact of high sample flow rates on the PAM molecular chains. This approach ensures the structural integrity of PAM, allowing it to effectively bridge and adsorb particles, thereby enhancing floc formation and settling. Combining PAC for initial coagulation and PAM for bridging and strengthening floc structure to achieve higher removal efficiency of pollutants through more defined solid–liquid separation provides an effective approach to optimizing the flocculation process.[33]

According to test results, the addition of PAM significantly improves the removal effect as monitored by various pollution indicators during the magnetic flocculation process (Fig. 1(i–l)). The COD removal efficiency initially rose and then declined with the gradual increase in PAM levels, peaking at 1 mg L^{-1} of PAM addition, with 70.56% $\pm$ 0.86% removal efficiency. The addition of PAM significantly improved the removal efficiency of suspended solids and NH$_3$-N, with maximal removal of 91.58% $\pm$ 0.41% and 21.35% $\pm$ 1.55%, respectively. TP removal efficiency increased and stabilized as more PAM was introduced.[34] The addition of PAM significantly enhances the removal efficiency of COD, SS, TP, and NH$_3$-N during magnetic flocculation treatment. The most significant impact was observed for COD removal. Quantitatively, PAM, as a high-molecular-weight organic polymer, exhibits a direct correlation between residual dosage and effluent COD elevation: experimental data showed that COD levels increased by 0.50 mg L^{-1}, 3.83 mg L^{-1}, and 1.59 mg L^{-1} at PAM dosages of 1.5 mg L^{-1}, 2 mg L^{-1}, and 2.5 mg L^{-1}, respectively, compared to the blank group. With the COD, the organic load increases at dosages exceeding 1 mg L^{-1} due to the accumulation of unflocculated residual PAM. When the dosage of PAM is 1 mg L^{-1}, the removal rates of COD, SS, and TP reach their highest, and the removal rate of TN also exceeds 20%. Its removal rate is not lower than that of higher doses (1.5–2.5 mg L^{-1}), balancing treatment efficiency and cost.

Additionally, the optimal dosage of PAM, as determined by Hu et al., is close to 1.74 mg L^{-1}.[35] However, excessive PAM addition increases the COD concentration in the water because it is an organic polymer. The optimal PAM addition amount was determined to be 1 mg L^{-1} based on a comprehensive consideration of the overall protocol.

3.2.4 **Determination of the optimal dosing sequence.** A systematic experimental design was constructed to determine the optimal chemical dosage sequence for the integrated magnetic flocculation-sedimentation device in actual operation, combining the application of PAC, magnetic powder, and PAM. The PAC, magnetic powder and PAM dosage was set to 60 mg L^{-1}, 100 mg L^{-1}, and 1 mg L^{-1}. Based on these conditions, four different chemical dosage sequence strategies were compared to establish the optimal dosing sequence during actual operation of the integrated magnetic flocculation-sedimentation device: (I) PAC-magnetic powder-PAM; (II) PAC-PAM-magnetic powder; (III) magnetic powder-PAC-PAM; and (IV) magnetic powder-PAM-PAC. The test results (Fig. SI2) indicated that the order of addition of the chemicals had a significant impact on the removal effect in the integrated magnetic flocculation sedimentation treatment process. The

magnetic powder → PAC → PAM sequence was the most effective. The main reasons for this sequential advantage when magnetic powder was added as the first step can be attributed to the following points: (1) it fully uses its significant specific surface area characteristics to initially adsorb pollutants in the water under physical action. The uniform distribution of magnetic powder laid a solid foundation for the subsequent flocculation process, ensuring complete contact between the magnetic powder and pollutants and initially forming a floc structure with the magnetic powder at its core. (2) Formation of magnetic core flocs: the early addition of magnetic powder not only facilitates the adsorption of pollutants but also enables the subsequent addition of PAC to react more effectively with the pollutants adsorbed by the magnetic powder, thereby forming a more compact and stable magnetic core floc. If magnetic powder were added later during the floc formation process, it could adhere only to the edge of the floc, resulting in an unstable magnetic floc structure and easy separation. (3) Avoiding magnetic powder aggregation: when magnetic powder and PAM are added simultaneously, the magnetic powder aggregates into clumps (viscous force) due to the high viscosity of the PAM solution. It cannot be evenly distributed in the water, thus affecting the magnetic flocculation effect. Therefore, adding magnetic powder before PAM can prevent this problem and ensure that the magnetic powder can maximize its role in adsorption and flocculation. Thus, the dosing sequence of magnetic powder → PAC → PAM fully leverages the advantages of physical adsorption by magnetic powder and the synergistic effect with chemical flocculants to form magnetic core flocs with a stable structure and high removal efficiency, significantly improving the treatment effect.

3.2.5 **Effect of hydraulic stirring conditions.** The hydraulic conditions in the flocculation process have an essential influence on the formation of flocs. The stirring speed should not be too high because a higher stirring speed breaks the formed flocs. Therefore, reasonable hydraulic conditions are essential to ensure floc formation. PAC, PAM and magnetic powder dosages were 60 mg L^{-1}, 1 mg L^{-1}, and 100 mg L^{-1}, respectively. The dosage order was first to add the magnetic powder, then PAC, and finally PAM. Under continuous test conditions, a four-factor, three-level orthogonal test was conducted on fast stirring speed, fast stirring time, slow stirring speed, and slow stirring time (see specific parameters in Table SI1). SPSS21.0 was used to design the L34 orthogonal test table.

3.2.5.1 Effect of hydraulic stirring conditions on COD removal efficiency. The influence of each factor on the COD removal efficiency was $A > B > D > C$; *i.e.*, fast stirring speed > fast stirring time > slow stirring time > slow stirring speed (Table SI1). The optimal theoretical combination was $A_2B_1C_2D_1$, *i.e.*, the fast-stirring speed, fast stirring time, slow stirring speed, and slow stirring time were 200 r min^{-1}, 1.5 min, 60 r min^{-1} and 4 min, respectively.

3.2.5.2 Effect of hydraulic stirring conditions on SS removal efficiency. The influence of each factor on the SS removal efficiency was $A > C > B > D$; *i.e.*, fast stirring speed > slow stirring speed > fast stirring time > slow stirring time (Table SI1). The optimal theoretical combination was $A_1B_2C_2D_2$, *i.e.*, the fast-

stirring speed, fast stirring time, slow stirring speed, and slow-stirring time were 100 r min^{-1}, 2 min, 60 r min^{-1} and 5 min, respectively.

3.2.5.3 Effect of hydraulic stirring conditions on TP removal efficiency. The influence of each factor on the TP removal efficiency was $A > D > B > C$; *i.e.*, fast stirring speed > slow stirring time > fast stirring time > slow stirring speed (Table SI1). The optimal theoretical combination was $A_2B_1C_1D_1$, *i.e.*, the fast-stirring speed, fast stirring time, slow-stirring speed, and slow stirring time were 200 r min^{-1}, 1.5 min, 40 r min^{-1} and 4 min, respectively.

3.2.5.4 Effect of hydraulic stirring conditions on ammonia nitrogen removal efficiency. The influence of each factor on the ammonia nitrogen removal efficiency was $A > B > C > D$; *i.e.*, fast stirring speed > fast stirring time > slow stirring speed > slow-stirring time (Table SI1). The optimal theoretical combination was $A_1B_3C_2D_1$; *i.e.*, the fast-stirring speed, fast stirring time, slow-stirring speed, and slow-stirring time were 100 r min^{-1}, 2.5 min, 60 r min^{-1} and 4 min, respectively.

The fast-stirring speed had a greater impact on the effect of pollutants, followed by the slow stirring time. In contrast, slow stirring speed and fast stirring time had less impact. In the fast-stirring stage, the agent must be thoroughly mixed with water quickly to disrupt the stability of the colloidal particles. This effectively increases the collision rate between particles, enhances the chance of collision and adsorption between magnetic species and destabilized flocs, and increases the degree of agglomeration of magnetic species. Under high stirring speeds, the agent and water mix quickly and thoroughly. Further growing the stirring time will weaken the strengthening effect of the agent and water. Therefore, the impact of the stirring speed on the mixing stage was greater than that of the stirring time. The slow stirring stage forms large particle flocs through the coagulant PAM, and the destabilized flocs are further destabilized through adsorption bridging, net capture, and sweeping.[36] The impact of slow stirring time on flocculation was greater than that of slow stirring speed, as the slow stirring speed plays a role in mixing the PAM molecules with the flocs without breaking up the formed flocs. When the slow stirring time was too long, the formed flocs were broken up, which was manifested in the loose floc bonding, resulting in high effluent COD, TP and SS. When the slow stirring time is too short, it becomes difficult to achieve the adsorption bridging of PAM molecules, which hinders the formation of flocs.[37] Therefore, the optimal hydraulic stirring conditions are a fast-stirring speed of 300 r min^{-1}, a fast-stirring time of 1.5 min, a slow stirring speed of 60 r min^{-1}, and a slow stirring time of 4 min.

3.2.6 Response surface optimization of magnetic flocculation treatment conditions. The single factors have certain connections and influences on one another. The response surface method was selected for subsequent investigation to study further the impact of each factor on the magnetic flocculation treatment effect. Response surface experiment design: based on the single-factor test results, the optimal ranges of the independent variables were determined to be PAC dosage (A), PAM dosage (B), and magnetic powder dosage (C). The COD removal efficiency (R1), SS removal efficiency (R2), TP removal

efficiency (R3), and ammonia nitrogen removal efficiency (R4) were taken as response values. The test factor level design and test results were analyzed using the Design-Expert 8.0.1 software (Table SI2).

3.2.6.1 COD removal efficiency (variance analysis). The binary polynomial model of COD removal efficiency and PAC (A), magnetic powder (B), and PAM (C) is: $Y = 68.46 - 1.0125 \times A + 1.5 \times B + 2.4375 \times C + 2.25 \times AB - 0.725 \times AC - 0.95 \times BC - 1.9425 \times A^2 - 2.7175 \times B^2 - 2.1425 \times C^2$, $R^2 = 0.9809$, $R^2_{adj} = 0.9563$. It can be seen from the variance analysis (Table SI2) that the P value of the model established based on the response value of COD removal efficiency was less than 0.0001. It showed that the experimental design is reasonable. The correlation coefficients $R^2 = 0.9809$ and $R^2_{adj} = 0.9563$ are similar, indicating that the actual value of the model is consistent with the predicted value. The lack of fit term is insignificant, indicating that the model fits the experimental data well, and the regression equation reflects the relationship between various factors and COD removal efficiency. A, B, C, AB, BC, A^2, B^2, and C^2 have high significance, indicating that the impact of each factor on COD removal efficiency is not a simple linear relationship. The influence of A, B, and C on the COD removal efficiency was $C > B > A$; *i.e.*, PAM > magnetic powder > PAC.

3.2.6.2 Interaction analysis. The RSM graph is a contour map of a three-dimensional space projected onto a two-dimensional plane, representing a specific response surface Y corresponding to the values of X1, X2, and X3. It intuitively reflects the influence of each factor on the response value. The interaction between the factors can be analyzed from the response surface analysis graph obtained.

When the dosage of PAC was fixed at 60 mg L^{-1}, the COD removal efficiency initially increased and then decreased with the increase in the dosage of magnetic powder, resulting in a significant overall change (Fig. 2). This indicates that the influence of magnetic powder on COD removal efficiency was greater than that of the PAC dosage. Similarly, the impact of PAM dosage on COD removal efficiency was greater than that of magnetic powder and PAC dosage. The AB and BC contour maps are elliptical, indicating that the interaction between the two was obvious. The interaction between the two factors significantly impacts COD removal efficiency, and the corresponding 3D surface diagram exhibits a more pronounced color change, with a relatively steep peak shape. The AC response surface is relatively flat, and the color change is not apparent, indicating that the interaction between the two is non-significant. These results are consistent with the variance analysis results in Table SI2. Optimal conditions are PAC 56.3 mg L^{-1}, magnetic powder 100.27 mg L^{-1}, and PAM 1.13 mg L^{-1}. These conditions were optimized to facilitate the test as PAC 56 mg L^{-1}, magnetic powder 100 mg L^{-1}, and PAM 1.0 mg L^{-1}. A verification test was conducted, and the COD removal efficiency was 71.2%, which was not significantly different from the predicted value of 69.4%.

3.2.6.3 SS removal efficiency (variance analysis). The binary polynomial model of SS removal efficiency and PAC (A), magnetic powder (B), and PAM (C) is: $Y = 91.3 - 0.6625 \times A +$
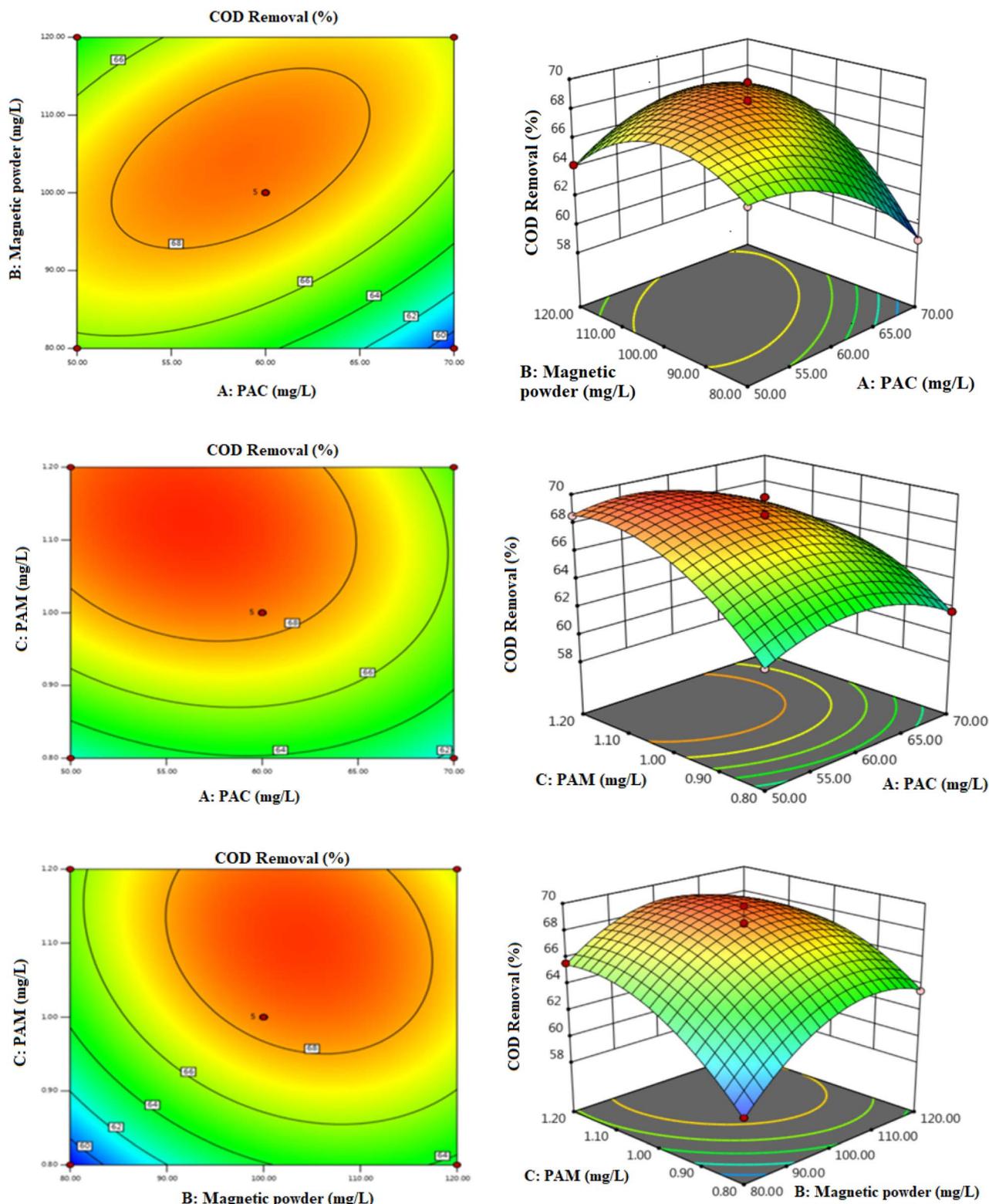
© 2026 The Author(s). Published by the Royal Society of Chemistry

Environ. Sci.: Adv., 2026, **5**, 753–771 | **759**

Fig. 2 Effect of interaction of various factors on the COD removal efficiency.

$1.7875 \times B + 2.5 \times C + 1.45 \times AB - 0.725 \times AC - 0.825 \times BC - 2.2 \times A^2 - 3.1 \times B^2 - 1.725 \times C$, $R^2 = 0.9743$, $R^2_{adj} = 0.9412$. The P-value of the model established with the response value of SS removal efficiency is less than 0.0001, indicating that the

experimental design is reasonable (Table SI2). The correlation coefficient R^2 (0.9809) is similar to R^2_{adj} (0.9563), indicating that the actual performance of the model value aligns closely with the predicted value.

The lack-of-fit term is insignificant, indicating that the model fits the experimental data well, and the regression equation accurately reflects the relationship between various factors and SS removal efficiency. The significance of B, C, AB, A^2, B^2, and C^2 is high, indicating that the influence of each factor on the SS removal efficiency is not a simple linear relationship. The influence of A, B, and C on the SS removal efficiency is $C > B > A$; *i.e.*, PAM > magnetic powder > PAC.

3.2.6.4 Interaction analysis. When the dosage of PAC was fixed at 60 mg L^{-1}, the SS removal efficiency first increased and then decreased with increasing dosage of magnetic powder, and the overall change was significant (Fig. 3). This showed that the influence of magnetic powder on SS removal efficiency was greater than that of the PAC dosage. Similarly, the impact of PAM dosage on SS removal efficiency was greater than that of magnetic powder and PAC dosage. The AB contour map is elliptical, indicating a strong interaction between the two. The interaction between the two factors significantly impacts the SS removal efficiency. The corresponding 3D surface map color changes are more pronounced, and the peak shape is relatively steep. The AC and BC contour plots are circular, the response surface is relatively flat, and the color change is not apparent. This demonstrates that the interaction between the two is not significant. These results are consistent with the variance analysis results in Table SI2. Optimal conditions are PAC 57.22 mg L^{-1}, magnetic powder 101.83 mg L^{-1}, and PAM 1.13 mg L^{-1}. The conditions were optimized to facilitate the test: PAC 57 mg L^{-1}, magnetic powder 102 mg L^{-1}, and PAM 1.0 mg L^{-1}. A verification test was conducted, and the SS removal efficiency was 93.1%, which was not significantly different from the predicted value of 92.4%.

3.2.6.5 TP removal efficiency (variance analysis). The binary polynomial model of TP removal efficiency and PAC (A), magnetic powder (B), and PAM (C) is: $Y = 89.6 - 0.6375 \times A + 1.875 \times B + 2.4375 \times C + 1.5 \times AB - 0.725 \times AC - 0.95 \times BC - 2.2375 \times A^2 - 3.0125 \times B^2 - 1.6875 \times C^2$, $R^2 = 0.9753$, $R^2_{adj} = 0.9435$. The P value of the model established based on the TP removal efficiency response value was less than 0.0001 (Table SI2). The experimental design is reasonable. The correlation coefficient R^2 (0.9753) is similar to R^2_{adj} (0.9435), indicating that the actual value of the model is consistent with the predicted value. The lack-of-fit term is insignificant, indicating that the model fits the experimental data well, and the regression equation accurately reflects the relationship between various factors and TP removal efficiency. The significance of B, C, AB, BC, A^2, B^2, and C^2 is relatively high. The influence of each factor on the TP removal efficiency is not a simple linear relationship. The influence of A, B, and C on the TP removal efficiency is $C > B > A$; *i.e.*, PAM > magnetic powder > PAC.

3.2.6.6 Interaction analysis. When the dosage of PAC was 60 mg L^{-1}, the TP removal efficiency initially increased and then decreased with increasing dosage of magnetic powder, resulting in a significant overall change. The impact of magnetic powder on TP removal efficiency is greater than that of the PAC dosage. The effect of PAM dosage on TP removal efficiency is greater than that of magnetic powder and PAC dosage. The AB and BC contour maps are elliptical, indicating a strong interaction

between the two (Fig. 4). The interaction between the two factors has a significant impact on the TP removal efficiency. The corresponding color change of the 3D surface map is more obvious, and the peak shape is steeper. The AC contour map is circular, the response surface is relatively flat, and the color change is not apparent. The interaction between the two is not significant. These results are consistent with the variance analysis results in Table SI2. Optimal conditions are PAC 57.47 mg L^{-1}, magnetic powder 102.224 mg L^{-1}, and PAM 1.14 mg L^{-1}.

The conditions were optimized to facilitate the test: PAC 57 mg L^{-1}, magnetic powder 102 mg L^{-1}, and PAM 1.0 mg L^{-1}. A verification test was conducted, and the TP removal efficiency was 91.2%, which was not significantly different from the predicted value of 90.7%.

3.2.6.7 Ammonia nitrogen removal efficiency (variance analysis). The binary polynomial model of ammonia nitrogen removal efficiency and PAC (A), magnetic powder (B), and PAM (C) is: $Y = 19.7 - 0.575 \times A + 1.8125 \times B + 2.5125 \times C + 1.55 \times AB - 0.8 \times AC - 0.825 \times BC - 2.0875 \times A^2 - 3.1125 \times B^2 - 1.7625 \times C^2$, $R^2 = 0.9695$, $R^2_{adj} = 0.9304$. The P-value of the model, established based on the ammonia nitrogen removal efficiency response value, is less than 0.0001 (Table SI2). This showed that the experimental design was reasonable. The correlation coefficient R^2 (0.9695) is similar to R^2_{adj} (0.9304), which indicates that the actual performance of the model values matches the predicted values. The lack of fit terms is insignificant, indicating that the model fits the experimental data well. The regression equation represents the relationship between various factors and ammonia nitrogen removal efficiency. The significance of B, C, AB, A^2, B^2, and C^2 is relatively high, indicating that the influence of each factor on ammonia nitrogen removal efficiency does not follow a simple linear relationship. The influence of A, B, and C on the ammonia nitrogen removal efficiency is $C > B > A$; *i.e.* PAM > magnetic powder > PAC.

Optimal conditions are PAC 57.55 mg L^{-1}, magnetic powder 102.39 mg L^{-1}, and PAM 1.14 mg L^{-1}. The conditions were optimized to facilitate the test: PAC 58 mg L^{-1}, magnetic powder 102 mg L^{-1}, and PAM 1.0 mg L^{-1}. The verification test showed that the ammonia nitrogen removal efficiency was 21.2%, which was not significantly different from the predicted value of 20.8%.

The optimal magnetic flocculation conditions based on the above four response surface test results are 57 mg L^{-1} of PAC, 102 mg L^{-1} of the magnetic powder, and 1.0 mg L^{-1} of PAM.

Under the optimum conditions, the highest COD, SS, TP, and ammonia nitrogen removal efficiencies reached 71.2%, 93.1%, 91.2%, and 21.2%, respectively.

3.2.6.8 Interaction analysis. When the dosage of PAC was 60 mg L^{-1}, the ammonia nitrogen removal efficiency first increased and then decreased with increasing dosage of magnetic powder, and the overall change was significant. The impact of magnetic powder on ammonia nitrogen removal efficiency is greater than that of the PAC dosage. Similarly, the effect of PAM dosage on ammonia nitrogen removal efficiency is greater than that of magnetic powder and PAC dosage (Fig. 5). The AB contour maps are elliptical, indicating that the

© 2026 The Author(s). Published by the Royal Society of Chemistry

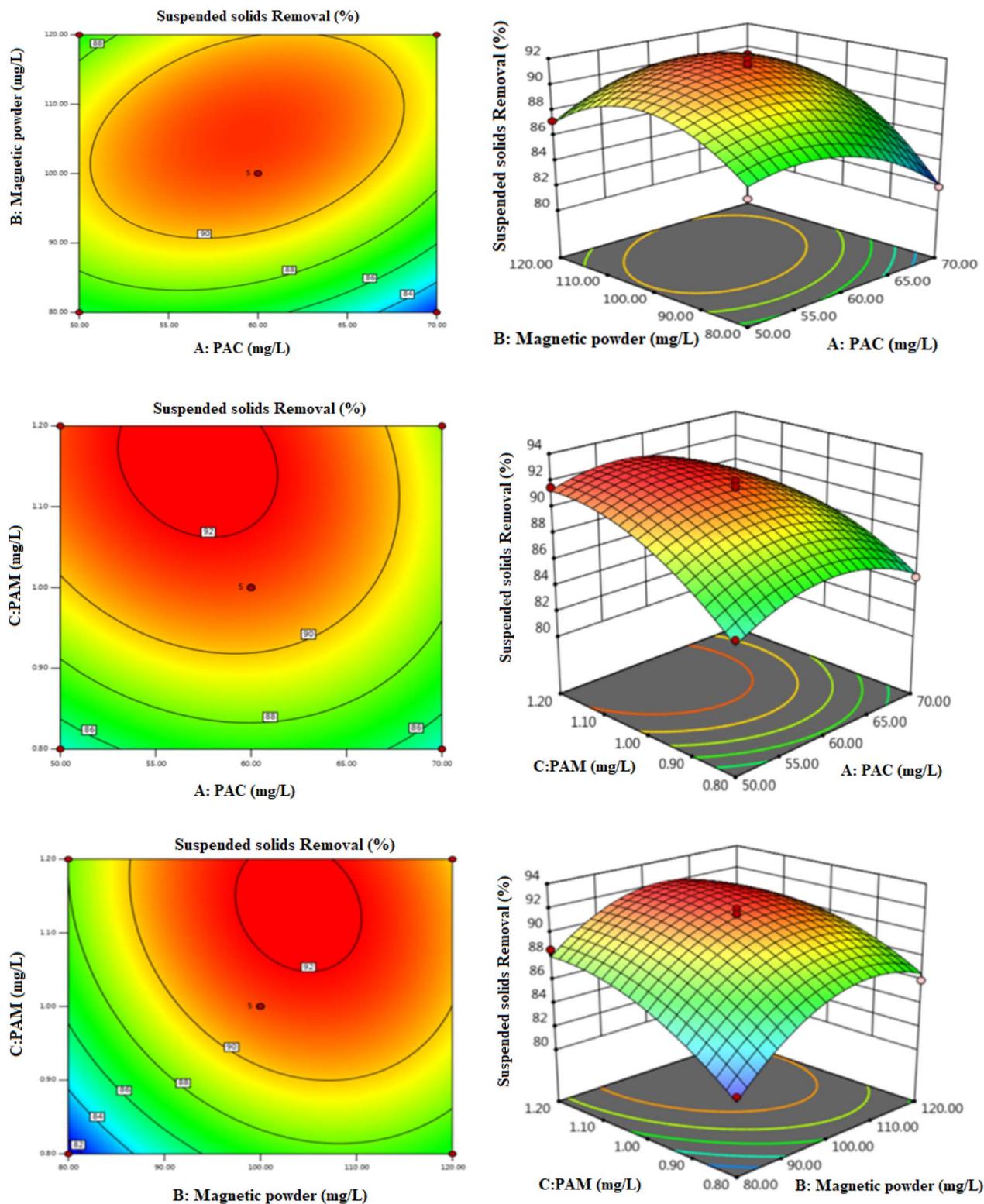*Environ. Sci.: Adv.*, 2026, **5**, 753–771 | **761**

Fig. 3   Effect of interaction of various factors on the suspended solids removal efficiency.

interaction between the two is obvious. The interaction between the two factors has a significant impact on the ammonia nitrogen removal efficiency. The corresponding 3D surface map colour change is more pronounced, and the peak shape is relatively sharper. The AC and BC contour map is circular, the response surface is relatively flat, and the color change is not apparent. The interaction between the two is not significant. These results are consistent with the variance analysis results in Table SI2.
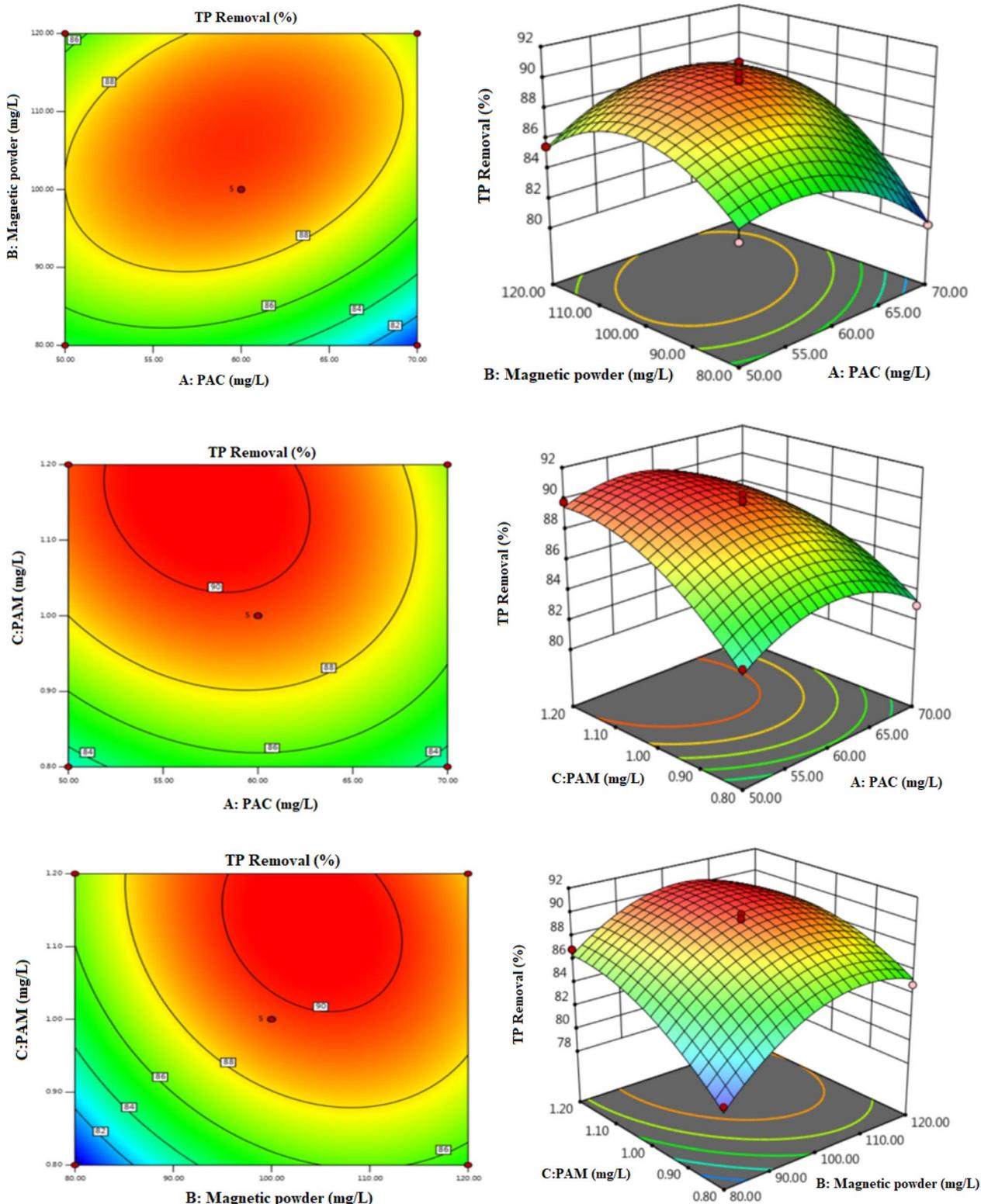
© 2026 The Author(s). Published by the Royal Society of Chemistry

Fig. 4   Effect of interaction of various factors on total phosphorous removal efficiency.

3.3 Actual operation effect and simulation of integrated flocculation-sedimentation treatment equipment

The design of the integrated flocculation sedimentation device is mainly based on the magnetic flocculation method and the horizontal tube sedimentation process. The device consists of a flocculation device and a sedimentation device. The designed water inlet flow rate is 4–8 m³ h⁻¹. The flocculation part includes the water inlet area and the first, second, and third

© 2026 The Author(s). Published by the Royal Society of Chemistry

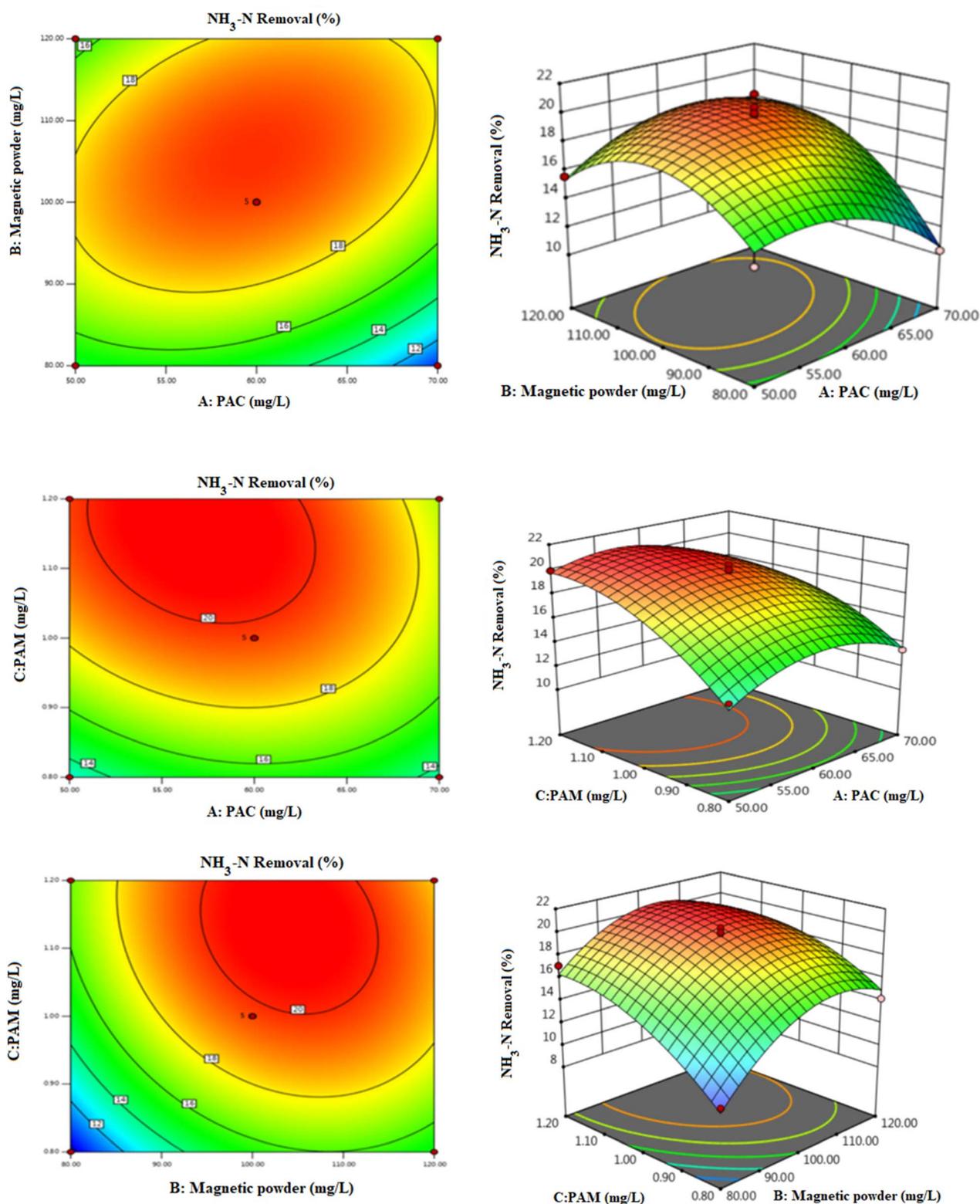Environ. Sci.: Adv., 2026, 5, 753–771 | 763

Fig. 5 Effect of the interaction of various factors on the ammonia nitrogen removal efficiency.

reaction tanks. The sedimentation part adopts a horizontal tube sedimentation tank, which is separated by a water distribution wall in the middle. Compared with the commonly used inclined tube sedimentation tank, the horizontal tube sedimentation tank effectively reduces the floor space. It improves the treatment efficiency (Fig. 6). The horizontal pipe sedimentation and

© 2026 The Author(s). Published by the Royal Society of Chemistry

separation part of the device consisted of 27 diamond-shaped horizontal pipes.

Each diamond-shaped pipe is 400 mm long, with a side length of 40 mm. The two lower sides of the diamond-shaped pipe formed a 60° angle with the horizontal plane, which helps the precipitated suspended matter to slide down when water flows through. At the 60° lower angle of each diamond-shaped pipe, multiple mud discharge ports are placed intermittently along the length direction. The width of the mud discharge port is 15 mm. When water flows into the diamond-shaped pipe, the precipitated suspended matter slides out of the mud discharge port along the two lower sides of the diamond. The slideway distance is very short, which avoids the accumulation of suspended matter in the diamond-shaped pipe and prevents blockage of the channel. The cross-sectional view of the horizontal tube sedimentation and separation device is shown in Fig. 6.

3.3.1 Operation effect of the device under different water volumes. The COD removal effect of the device was apparent under different water volumes. When the water volume was 4 $m^3 h^{-1}$ and 6 $m^3 h^{-1}$, the average COD removal efficiencies were 82.06% and 72.67%, respectively. Under these two water inflows, the maximum effluent COD concentration did not exceed 20 mg L^{-1} over 30 days of operation. However, when the water inlet volume was increased to 8 $m^3 h^{-1}$, maximum COD removal efficiency dropped to 59.96% ± 2.50%. The fluctuation trend of COD removal efficiency gradually increased as the water inlet volume increased (Fig. 7). The magnetic flocculation

process utilizes magnetic powder to enhance the adsorption bridging of the flocculant, compress the double electric layer, and create an entrapment effect, causing COD in the water to become unstable, collide, and agglomerate to form flocs. The sedimentation effect of the horizontal settling tube then separates the particles from the water, thus achieving water purification. However, in this study, COD removal mainly relied on the physical adsorption of magnetic powder and its chemical interaction with the flocculant, without the involvement of microbial degradation. Furthermore, considering that the coagulant PAM itself is organic, the addition of PAM also increased the COD concentration to some extent. The optimized dosage and dosage methods of the magnetic powder, PAC and PAM are discussed in Section 3.2. The COD removal efficiency of high-purity Fe_3O_4 magnetic powder is closely related to its application form (*e.g.*, alone or as a composite) and the water quality. Its cost advantage mainly comes from recyclability, which offsets the initial material expense. In addition, high-purity Fe_3O_4 itself has limited direct COD removal ability; therefore, it is usually used in modified or composite forms to enhance its efficiency. The cost of regeneration (physical or chemical) is also related to expenses. Taking 15 cycles of reuse (mild wastewater scenario) as an example, the total cost per ton of water is approximately $0.3–4.

Based on the optimized dosage and dosing method of magnetic powder, PAC, and PAM obtained in Section 3.2, an integrated horizontal tube sedimentation unit was designed as the test platform, and dredged sludge residual water was used
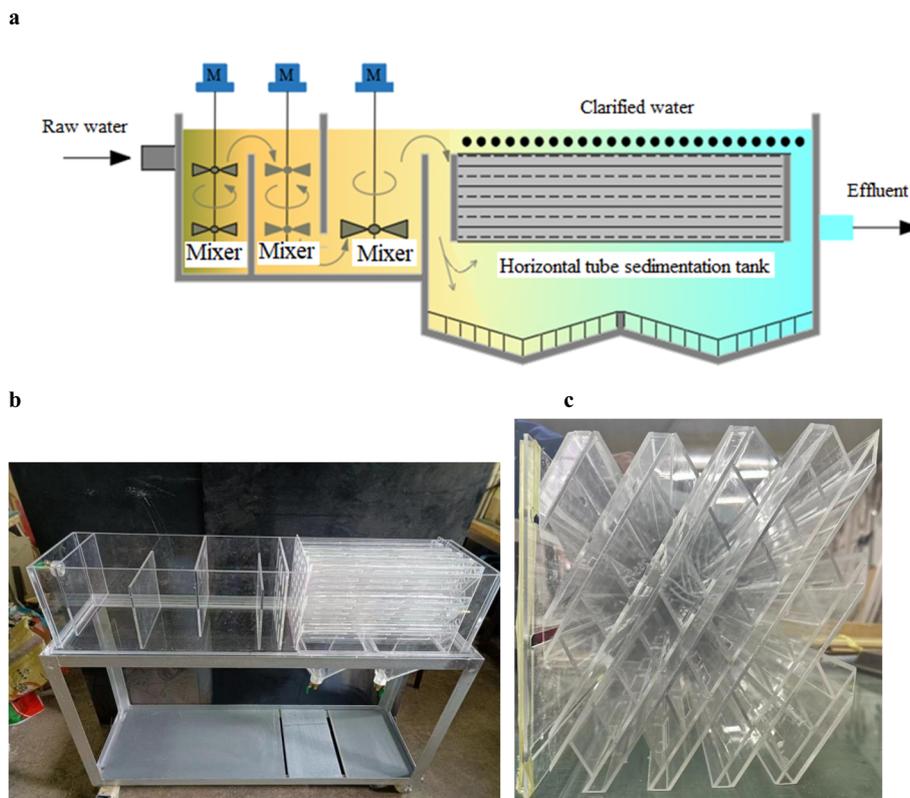

Fig. 6 (a) Schematic of the device; (b) photographic image of the device in the laboratory, and (c) a cross-sectional view of the horizontal tube of the sedimentation separation device.

© 2026 The Author(s). Published by the Royal Society of Chemistry
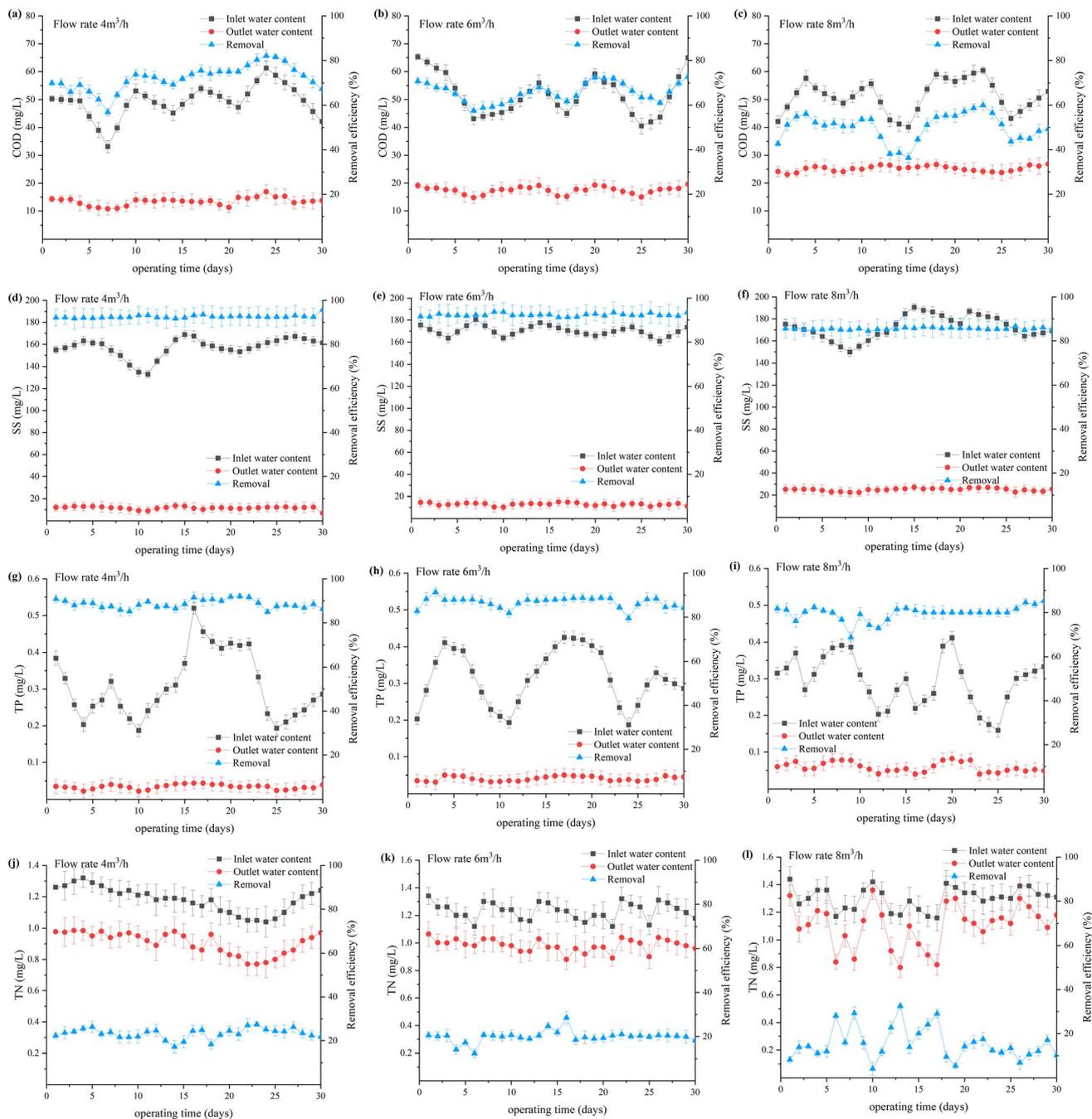
Environ. Sci.: Adv., 2026, **5**, 753–771 | **765**

Fig. 7 Removal effect of: (a–c) COD, (d–f) suspended solids, (g–i) total phosphorous, and (j–l) total nitrogen inside the device.

as the treatment object to investigate the treatment effect of the device on wastewater under different continuous influent volumes. The results showed that when the water volume was 4 m^3 h^{-1}, the device had a stable and good SS treatment effect (average SS removal efficiency 92.59% and maximum removal efficiency 95.74% $\pm$ 3.94%) during the 30 day operation period. There was no significant difference in the SS removal efficiency when the water volume was 6 m^3 h^{-1} (average SS removal efficiency 92.39%, and maximum removal efficiency 93.79% $\pm$ 3.04%) (Fig. 7). However, when the water inlet volume was increased to 8 m^3 h^{-1}, the removal effect decreased. The average and maximum SS removal rates were 85.52% and 86.37% $\pm$

3.75%, respectively. When the water inlet volume was high, the contact and reaction time between the flocculant and the suspended matter was insufficient, considering that the flocculation reaction time is closely related to the flocculation effect. The improvement in the flocculation effect by magnetic powder and coagulant aids was gradually limited. It can be reasonably inferred that with the further increase of the water inlet volume, the removal effect of SS will further decrease. Compared with conventional sedimentation, magnetic flocculation + horizontal tube sedimentation has a higher energy efficiency and reduces sludge production.[38]

766 | *Environ. Sci.: Adv.*, 2026, 5, 753–771

© 2026 The Author(s). Published by the Royal Society of Chemistry

As the influent rate increased, the device's TP removal efficiency followed a similar trend to that of SS and COD. With increasing water flow, TP removal efficiency gradually decreased (Fig. 7). At influent rates of 4 m^3 h^{-1} and 6 m^3 h^{-1}, the device's TP removal efficiency showed minimal difference, with average removal rates of 89% and 87.18%, respectively. Effective TP removal was achieved in both cases. Over 30 days of operation, the effluent TP concentration did not exceed 0.2 mg L^{-1}, meeting the limit for the Surface Water Environmental Quality Standard.[32,33] When the influent rate was increased to 8 m^3 h^{-1}, the device's average and maximum TP removal rates were 80% and 85.29% ± 2.01%, respectively. At an influent flow rate of 8 m^3 h^{-1}, the effluent TP concentration remained within the standard limit requirement for surface water, indicating that the device achieved satisfactory TP removal at all influent flow rates. However, considering the device's performance in removing SS and COD, at a flow rate of 8 m^3 h^{-1}, the device did not achieve overall water quality compliance; 6 m^3 h^{-1} was the highest influent flow that met the required limits of the test.

As the influent flow rate was increased, the NH$_3$-N removal efficiency of the device changed similarly to that of COD. As the water volume was increased, the removal effect of NH$_3$-N by the device changes similarly to that of COD. When the water inflow was 4 m^3 h^{-1}, 6 m^3 h^{-1} and 8 m^3 h^{-1}, the average NH$_3$-N removal efficiency was 23.26%, 20.01%, and 15.07%, respectively. Furthermore, as the water flow rate increased, the removal rate changed from a stable trend to a significant fluctuation (Fig. 7). When the water volume was 4 m^3 h^{-1} and 6 m^3 h^{-1}, the effluent NH$_3$-N concentration basically met the limit requirements of the Surface Water Environmental Quality Standard[39,40] during 30 days of operation. This indicates that it is challenging to efficiently treat NH$_3$-N at higher water volumes by relying solely on adsorption and enhanced magnetic flocculation. Table 2 shows the changes in sedimentation tank operating parameters under different treatment rates. As the treatment rate increases, the overflow load gradually increases, reducing the flocculation, sedimentation, and total residence time. Therefore, considering the rationality of design, the economic efficiency of investment and construction, and the high efficiency of actual operation, the optimal overflow load of the sedimentation tank was determined to be 15.5 (m^3 (m^{-2} h^{-1})).

3.3.2 Simulation study of the device

3.3.2.1 Simulation model. The test device is modeled in three dimensions through the pre-processor space claim. Simulation technology was used to simulate and analyze the various working conditions of the device, thereby reducing the consumption of workforce and material resources. It can effectively avoid the impact of operational errors during the test. The test device is modelled 1 : 1. The specific model is shown in Fig. 8a and b. The device model consists of two main parts: a flocculation tank and a sedimentation tank. The interior includes a water inlet, a flocculation baffle, a water distribution wall, a horizontal pipe structure, a mud sliding area structure, and a water outlet, among other components. The total length of the model is 1100 mm, and the width is 255 mm, of which the length of the flocculation area is 500 mm, the length of the

Table 2 Operating parameters of the sedimentation tank under different treatment volumes

Operating parameters	Treatment water volume		
	4 m^3 h^{-1}	6 m^3 h^{-1}	8 m^3 h^{-1}
Overflow load (m^3 (m^{-2} h^{-1}))	11.2	15.5	18.3
Flocculation time (min)	6.5	4.3	3.7
Sedimentation time (min)	2.1	1.5	0.9
Total residence time (min)	9.2	7.2	5.8

horizontal pipe sedimentation tank area is 500 mm, and the overall depth of the device is 250 mm.

3.3.2.2 Divide the grid (meshing). This model utilizes the built-in mesh processor, fluent meshing in the fluent processor for meshing. The number of grids was 1574281. The local and overall effects of the model grid are illustrated in Fig. 8c and d. The Elements were set to Tet/Hybrid, Type to Hex Core (Native), Offset layers to 4, and Interval size to 10. The quality of the grid was checked through the console panel. The EquiSize Skew (indicated skewness) was less than 0.65, and the Aspect ratio (aspect ratio of the grid) was less than 3.5. This showed that the meshing quality meets the requirements. The MESH file was exported for subsequent simulation calculations.

3.3.2.3 Determination of boundary conditions. (i) *Inlet flow rate*: according to laboratory tests at room temperature, the impurity density of the dredged residual water was 1050 kg m^{-3}, and the dynamic viscosity of the impurities was 0.02 Pa s. The actual operating flow rate of the device was 5 m^3 h^{-1}, which was converted into the inlet velocity. The calculation formula is shown in (eqn (1)):

$$v = \frac{4Q_V}{\pi D_{in}{}^2} \tag{1}$$

According to this formula, the inlet flow velocity of the water inlet of the integrated device was 0.044 m s^{-1}.

(ii) *Impurity ratio*: the impurities in the dredging residual water are mainly suspended sludge particles, which are often represented by SS in sewage testing. The flocculant PAC was added to the water to facilitate the formation of flocs during the flocculation stage. The agent reacts physically and chemically with water and impurities, which is beneficial for removing impurities. Floc is converted into an impurity concentration in the simulation analysis. The impurity ratio was 10% after conversion.

(iii) *The following assumptions are made to facilitate simulation calculations*: it is assumed that the fluid in the device is a Newtonian fluid and that no temperature changes occurred when the chemical agent reacts with water and impurities, and the energy loss of water flow from the starting point to the endpoint was ignored.

3.3.2.4 Specific analysis. A numerical simulation study was conducted on an integrated flocculation-sedimentation wastewater treatment device with water inlet velocities of 0.022 m s^{-1}, 0.044 m s^{-1} and 0.088 m s^{-1}. By varying the water inlet velocity,

© 2026 The Author(s). Published by the Royal Society of Chemistry

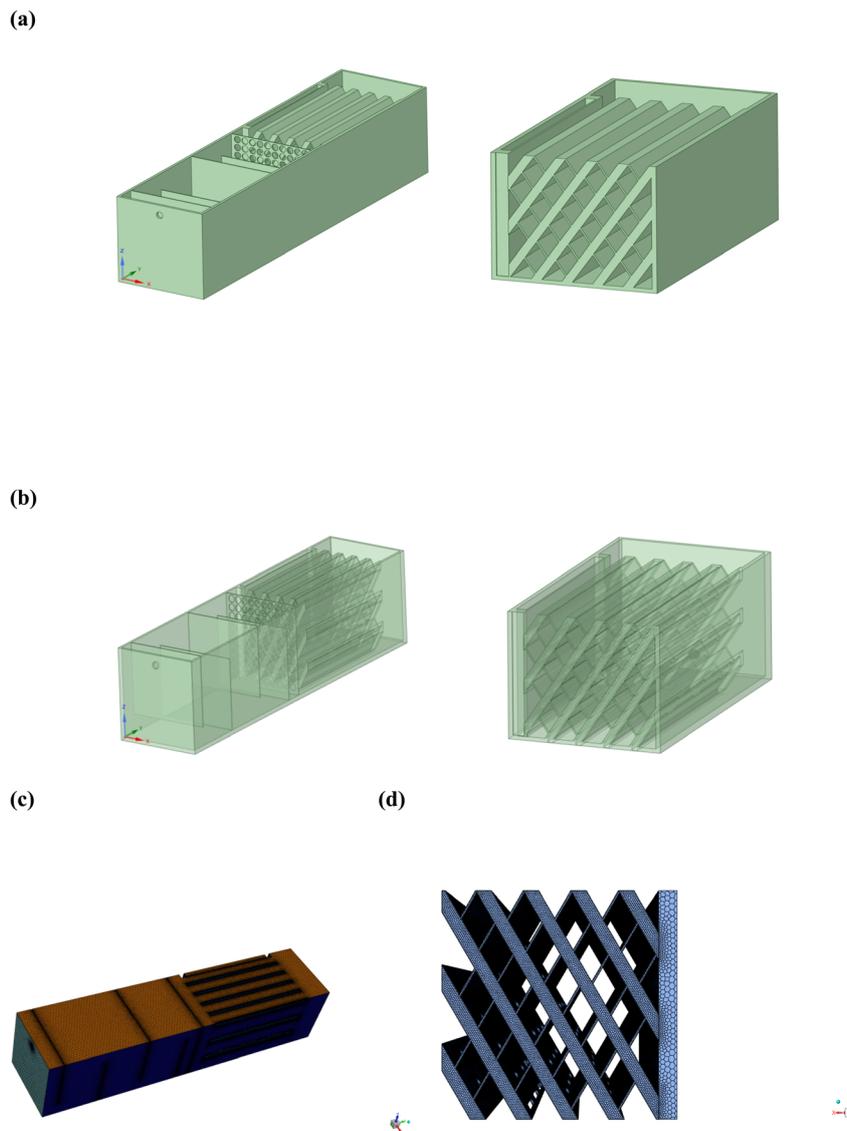*Environ. Sci.: Adv.*, 2026, **5**, 753–771 | **767**

Fig. 8 Test device: (a) 3D model, (b) perspective view of the 3D model, (c) grid structure diagram, and (d) cross-sectional view of the grid.

the changes in the flow field within the device and the sedimentation distribution were studied.

(i) *Flow velocity distribution*: flow velocity distribution is one of the key factors affecting the treatment effect in an integrated flocculation-sedimentation wastewater treatment device. Reasonable flow velocity distribution is crucial for the effective sedimentation of impurities.[41] The flow velocity distribution within the device at various water inlet velocities was analyzed using numerical simulation. Velocity cloud diagrams analyze flow velocity distribution. The water phase velocity cloud diagram at the $X = 0$ section and $Z = 0.085$ section at different velocities is shown in Fig. SI3. It can be seen from the numerical simulation results that when the water inlet velocity was 0.022 m s^{-1}, the velocity distribution inside the equipment was relatively uniform and the water flow velocity was moderate, which was conducive to the sedimentation of impurities. The velocity distribution inside the equipment became complex when the water inlet velocity was increased to 0.044 m s^{-1} and

0.088 m s^{-1}. Higher velocity appears in some areas, which may have an adverse effect on the sedimentation of impurities. To understand the impact of velocity distribution on impurity sedimentation, the average velocity, average turbulent kinetic energy, and average turbulent kinetic energy dissipation rate inside the equipment were further analyzed (Table 3).

The average turbulent kinetic energy and average turbulent kinetic energy dissipation rate increased as the water inlet speed and the average speed inside the equipment gradually increased. This means that the turbulence of the water flow inside the equipment increases, which may have an adverse effect on the sedimentation of impurities.[42]

(ii) *Pressure distribution*: pressure distribution is one of the critical indicators for evaluating the operational stability of integrated flocculation-sedimentation sewage treatment equipment. Pressure distribution not only affects the flow field characteristics inside the equipment but is also closely related to the structural strength and sealing performance. The

Table 3 Average velocity, average turbulent kinetic energy, and average turbulent kinetic energy dissipation rate inside the device at different speeds

Inlet velocity (m s^{-1})	Average velocity (m s^{-1})	Average turbulent kinetic energy (m^2 s^{-2})	Average turbulent kinetic energy dissipation rate (m^2 s^{-3})
0.022	0.00155	1.29×10^{-6}	2.01×10^{-6}
0.044	0.00210	2.05×10^{-6}	4.29×10^{-6}
0.088	0.00287	3.45×10^{-6}	9.27×10^{-6}

pressure distribution cloud map of different cross-sections within the equipment can be obtained through numerical simulation (Fig. SI4). According to the numerical simulation results above, the pressure distribution inside the equipment changes to a certain extent with the increase in water inlet velocity. When the water inlet velocity was 0.022 m s^{-1}, the pressure distribution inside the equipment was relatively uniform, and there was no pronounced pressure gradient. However, when the water inlet velocity increased to 0.044 m s^{-1} and 0.088 m s^{-1}, the pressure distribution inside the equipment became uneven, and higher-pressure gradients appeared in some areas. The presence of this pressure gradient may adversely affect the structural strength and sealing performance of the equipment.[43] It was observed from the inlet and outlet pressure drop–velocity curve (Fig. SI5) that as the water inlet and outlet pressure drops increase, the pressure drops at the inlet and outlet of the equipment increase accordingly. This showed that the resistance of the water flow inside the equipment increases, which may affect the operational stability and treatment effect of the equipment.

(iii): *Impurity distribution*: in the numerical simulation of this present study, we focused on the impurity distribution inside the equipment at different water inlet velocities. The impurity distribution diagram of the $X = 0$ section and $Z = 0.085$ section under different inlet velocities is shown in Fig. SI6. It can be seen from the numerical simulation results that when the water inlet speed was 0.022 m s^{-1}, the impurities were well-settled inside the equipment. Most of the impurities are concentrated at the bottom of the equipment, indicating that the equipment has a good sedimentation effect at this speed. However, when the water inlet velocity was increased to 0.044 m s^{-1} and 0.088 m s^{-1}, the distribution of impurities inside the equipment became more uniform, and some impurities did not settle effectively to the bottom of the equipment. This showed that a higher water inlet velocity may adversely affect the equipment's sedimentation effect.

4 Conclusion

In response to the pollution problems of rivers and lakes in recent years, the use of environmentally friendly dredging and ecological restoration methods that can effectively treat the endogenous pollution in polluted water bodies has accelerated. This study is based on the environmental dredging project of Wolong Lake Wetland. To restore the ecological environment of Wolong Lake Wetland, the selection of reagents, dosage and

treatment methods for dredged sludge residual water in the Wolong Lake area was studied. PAC, PFS, FeCl$_3$ and Al$_2$(SO$_4$)$_3$ were used as flocculants to treat the residual water from dredged sludge. PAC treatment of the dredged sludge wastewater at a dosage of 60 mg L^{-1} was better than the other three flocculants. The addition of magnetic powder at the start of the process is more conducive to pollutant removal. Reagents are added in the following order: flocculant PAC is added immediately after magnetic powder, followed by coagulant PAM with brief stirring. The treatment effect is optimal when the magnetic powder particle size is 45 μm. Hydraulic conditions for the optimal magnetic flocculation effect include adding 100 mg L^{-1} of magnetic powder, stirring rapidly for 1.5 minutes at 300 rpm, adding 60 mg L^{-1} of PAC, and adding 1 mg L^{-1} of PAM at a slow speed of 60 rpm, and stirring for four minutes. Once the stirring is finished, the liquid is allowed to stand for 20 minutes. The response surface results indicate a significant interaction among the three factors. The designed and developed integrated sewage treatment equipment operated continuously for 30 days at varying water inflows of 4 m^3 h^{-1}, 6 m^3 h^{-1}, and 8 m^3 h^{-1}. The study found that the device has a significant impact on COD, SS, TP, and NH$_3$-N levels. The removal effect gradually decreases as the water flow rate increases. Combined with the operating parameters of the sedimentation tank under different water volumes, the integrated system achieved >90% removal of SS and TP with an optimal overflow load of 15.5 (m^3 (m^{-2} h^{-1})). Under these conditions, the device's COD, SS, TP, and NH$_3$-N effluent meet the surface water limit of the Surface Water Environmental Quality Standard (GB 3838-2002), and the equipment operates stably. Through numerical simulation, the study found that as the water inlet velocity increased, the flow velocity distribution inside the equipment became more complex, and higher flow velocities and pressure gradients appeared in certain areas. This could adversely affect the sedimentation of impurities. At the same time, at a higher water inlet velocity, the distribution of impurities inside the equipment became more uniform, and the sedimentation effect decreased. This study lays the foundation for treating dredged sludge residual water through an integrated magnetic flocculation-horizontal tube sedimentation process. This study has environmental relevance, contributing to the restoration and reuse of Wolong Lake's sediment. Environmentally friendly dredging and ecological restoration methods can effectively treat the endogenous pollution of polluted water bodies.

Further work is being conducted in our laboratory to investigate the recovery rate of magnetic powder after magnetic

© 2026 The Author(s). Published by the Royal Society of Chemistry

Environ. Sci.: Adv., 2026, **5**, 753–771 | **769**

flocculation treatment and the mechanism of pollutant removal in terms of magnetic flocculation technology. With the continuous development and progress of dredging technology and magnetic flocculation technology, theoretical research on the treatment of bottom mud residual water in environmental protection dredging, as well as its application in practical engineering, will become more extensive. Building on the successful application of the integrated magnetic flocculation-horizontal tube sedimentation process for treating dredged sludge effluent in the Wolong Lake environmental dredging project, future research will focus on three key directions: conducting adaptability tests tailored to the water quality characteristics of other eutrophic lakes to verify the process's universality; enhancing long-term operational stability by optimizing equipment anti-interference capabilities and wear control; and exploring on-site large-scale automation potential through intelligent sensing to achieve full-process precise control, thereby promoting the broad application of this efficient integrated treatment scheme in lake environmental dredging projects and providing technical support for eutrophic water remediation.

Conflicts of interest

There are no conflicts to declare.

Data availability

The data supporting this article have been included as part of the supplementary information (SI). Supplementary information is available. See DOI: https://doi.org/10.1039/d5va00297d.

Acknowledgements

References

1 L. Yu, Discussion on environmentally friendly dredging sediment yard residual water treatment methods and implementation devices, *Green Environmentally Friendly Building Materials*, 4, 2018.

2 C. Fan, M. Liu and S. Wang, Research progress and prospects on sediment environment and pollution control in my country in the past 20 years, *Prog. Earth Planet. Sci.*, 2021, **36**, 346–374.

3 D. Dai, S. He, X. Chen, F. Yang and K. Hainan, Study on improving the dehydration and drying efficiency of environmentally friendly dredged bottom mud, *J. Environ. Eng.*, 2013, **7**, 1901–1906.

4 Qi Wang and L. Zhonghua, Study on environmentally friendly dredging sediment yard residual water treatment

5 X. Zheng and H. Yinghao, Application cases of magnetic loading multi-effect clarification technology in urban black and odorous water treatment and urban domestic sewage treatment, *J. Environ. Eng.*, 2021, **15**, 3136–3142.

6 J. Liu, T. Guangduo, L. Zenan, Li Dong and L. Hailong, Mechanism design of flat-plate magnetic separation equipment for sewage treatment, *Mach. for Machinery*, 2022, **60**, 13–16.

7 H. P. Hong, H. W. Kwon, J. J. Kim, D. W. Ha and Y. H. Kim, Magnetic force assisted settling of fine particles from turbid water, *Prog. Supercond. Cryog.*, 2020, 7–11.

8 H. Huaihuai, SediMag~(TM) magnetic flocculation sedimentation for wastewater treatment standard improvement and deep phosphorus removal, *China Water Supply and Drainage*, 33, 2017, 53–56.

9 N. Y. Arifpin and I. Alfadila, in *Wastewater Treatment Process for Removing Chemical Oxygen Demand*, Google Patents, 2019.

10 F. Wang, S. Foucher, J. I. Zhouying and F. Liu, in *Wastewater Treatment Process for Removing Chemical Oxygen Demand*, Google Patents, 2020.

11 D. A. Potts, in *Wastewater Leaching System*, Google Patents, 2017.

12 M. Kumari and S. K. Gupta, A novel process of adsorption cum enhanced coagulation-flocculation spiked with magnetic nanoadsorbents for the removal of aromatic and hydrophobic fraction of natural organic matter along with turbidity from drinking water, *J. Clean. Prod.*, 2020, **244**, 118899.

13 M. Stolarski, C. Eichholz, B. Fuchs and H. Nirschl, Sedimentation acceleration of remanent iron oxide by magnetic flocculation, *China Particuology*, 2007, **5**, 145–150.

14 L. Jia, Li Zhen and J. Shaoyi, Application of magnetization technology in industrial water treatment, *Chem. Ind. Eng.*, 2006, **1**, 59–64.

15 H. Zhao and J. Wang, Study on treating urban sewage using magnetic flocculation method, *J. Lanzhou Railway Inst.*, 2002, **3**, 79–82.

16 S. J. Langer, R. Klute and H. H. Hahn, Mechanisms of floc formation in sludge conditioning with polymers, *Water Sci. Technol.*, 1994, **30**, 129.

17 S. Xue and Z. M. e. al. Wen Yukun, Engineering application of horizontal tube high-efficiency sedimentation tank in the expansion of water treatment plant, *Water Pur. Technol.*, 2022, **41**, 154–160.

18 Q. Zhong and X. Gaozong, A brief discussion on the application and progress of environmentally friendly dredging technology/Chinese Society for Environmental Science, in *Proceedings of the 2013 Academic Annual Conference of the Chinese Society for Environmental Science*, CCCC Shanghai Waterway Survey and Design Institute Co., Ltd, 5, 2013.

19 F. Chengjun, Process design of large-scale water plant expansion project in Feidong County, Anhui, *China Water Supply and Drainage*, 35, 2019, 41–44.

20 J. Tang and F. Sumei, Application of horizontal tube high-efficiency sedimentation technology in sewage Class A treatment, *Chin. Environ. Dev.*, 2018, **30**, 101–102.

methods and implementation devices, *J. Water Resour. Hydraul. Eng.*, 2012, **23**, 179–181.

21 J. Bridgeman, B. Jefferson and S. A. Parsons, Computational fluid dynamics modelling of flocculation in water treatment: a review, *Eng. Appl. Comput. Fluid Mech.*, 2009, **3**(2), 220–241.

22 L. K. Wang and M. H. S. Wang, A New Wave of Flotation Technology Advancement for Wastewater Treatment. in *Environmental Flotation Engineering. Handbook of Environmental Engineering*, ed Wang, L. K., Wang, M. H. S., Shammas, N. K., Aulenbach, D. B., Springer, Cham, 2021, 21, DOI: 10.1007/978-3-030-54642-7_4.

23 J. A. M. Alegría, E. M. España and J. F. F. Marulanda, Dissolved Air Flotation: A Review from the Perspective of System Parameters and Uses in Wastewater Treatment, *Rev. Tecnol.*, 2021, (52), 2111.

24 L. Peng, Analysis of plant diversity in Wolong Lake Nature Reserve in Shenyang City, *Environmental Protection and Circular Economy*, 2018, 6, 34–38.

25 H. He and C. Gao, Synthesis of Fe3O4/Pt Nanoparticles Decorated Carbon Nanotubes and Their Use as Magnetically Recyclable Catalysts, *J. Nanomater.*, 2011, 10, DOI: 10.1155/2011/193510.

26 A. D. Eaton, L. S. Clescen, E. W. Rice and A. E. Greenberg, in *APHA. Standard Methods for the Examination of Water & Wastewater*, American Public Health Association, American Water Works Association, Water Environment Federation, 2005.

27 K. Zheng and Y. Hong, Application of flocculants in sewage treatment, *Cleaning the World*, 2020, 36, 106–107.

28 D. Gao, Q. Jia and S. Yabin, Research progress on the application of flocculants in water treatment, *Papermaking Equipment and Materials*, 2022, 51, 88–90.

29 L. Zhonghe, in *Research and Application of Key Technologies for Treating Aquaculture Wastewater with Magnetic Flocculation and Microbial Preparations*, Jilin Academy of Agricultural Sciences, China, 2021.

30 L. Yinong, X. Jianhua and S. Bin, *Technical Analysis of a Coupled Precipitation System for Magnetic Particle Heavy Media, Modern Industrial Economics and Informatization*, 2021, 11, 63–64.

31 L. Xiaomin, Research on the application of magnetic flocculation sedimentation process in wastewater treatment, *Leather Manufacturing and Environmental Protection Technology*, 2021, 2, 87–88.

32 Z. Yu, in *Experimental Study on Magnetic Flocculation for Urban Sewage Emergency Treatment*, Xihua University, China, 2021.

33 X. Dai, in *Application of Electrochemical Ion-Adjusted Cyclonic Magnetic Flocculation Technology in Oilfield Wastewater Treatment*, Yanchang Oilfield Co., Ltd, Qilicun Oil Production Plant, Shaanxi Province, 2021.

34 C. Xinquan, in *Research on the Combined Treatment of Simulated Dye Wastewater by Electrocoagulation and Electrocoagulation and Magnetic Flocculation*, Dalian Maritime University, China, 2020.

35 J. W. Hu, J. Li, F. Q. Yu, C. W. W. Wang and G. Y. Liu, Analysis of magnetic flocculation process conditions for river water treatment by response surface method, *J. Beijing Univ. Technol.*, 2013, **39**(3), 459–465.

36 Z. Duan and Li Yan, Li Guangzhu, Advanced treatment of domestic sewage by magnetic flocculation, *China Rural Water Conservancy and Hydropower*, 2019, **07**, 110–118.

37 Z. Dong, R. Weigen and C. Rong, Design and application of magnetic seed micro-flocculation strong magnetic separation and purification technology in mine wastewater treatment, *Coal Engineering*, 2013, **45**, 22–24.

38 E3S Web of Conferences, Application of Magnetic Coagulation Sedimentation Tank and Sand-adding High-efficiency Sedimentation Tank in Sewage Treatment, 2025, https://www.e3sconferences.org/articles/e3sconf/pdf/2025/17/e3sconf_eeupd2024_01007.pdf.

39 USEPA, US Environmental Protection Agency (USEPA), in *Nutrient Criteria Technical Guidance Manual: Lakes and Reservoirs*, Environmental Protection Agency, Office of Water, Washington, DC, EPA822-B00-001., 2000.

40 *Environmental quality standards for surface water*, M. E.T. PRC, GB3838-2002 National Standard of The People's Republic of China, 2002.

41 W. Jian, *Research on Transient Flow Characteristics of Pipelines Based on CFD*, in, Zhejiang University, China, 2019.

42 C. Xiuhua, in *Research on CFD Model Construction and Prediction Analysis of Spatial and Temporal Distribution of Greenhouse Environmental Factors*, Jiangsu University, Zhenjiang, China, 2011.

43 H. Feng, Computational Fluid Dynamics Analysis CFD Software Principles and Applications, Master thesis, Tsinghua University Press, Beijing China, 2023, pp. 30–35.

© 2026 The Author(s). Published by the Royal Society of Chemistry

Environ. Sci.: Adv., 2026, **5**, 753–771 | **771**